Electronic Structure of Nitrosyl Ferrous Heme Complexes

Ahmad Waleh,*,† Nan Ho,† Lek Chantranupong,† and Gilda H. Loew†,‡

Contribution from The Molecular Theory Laboratory, The Rockefeller University, 701 Welch Road, Suite 213, Palo Alto, California 94304, and SRI International, 333 Ravenswood Avenue, Menlo Park, California 94025. *Received March 28, 1988*

Abstract: The results of a generalized open-shell treatment of the ground-state electronic structure of nitrosyl ferrous heme complexes, within the framework of a semiempirical INDO-SCF (intermediate neglect of differential overlap) procedure, are presented. The results demonstrate the existence of two distinct, low-energy electronic states corresponding to the formal assignment of the unpaired electron to either NO or iron atomic orbitals. It is shown that these two states are nearly degenerate at axial ligand distances close to the observed values in heme protein complexes. It is further shown that both the extent of degeneracy and the relative energy order of the two electronic states are sensitive to minor changes in the axial ligand bond distances and angles. The implications of these results provide a coherent interpretation of the observed EPR spectra of complexes of NO with various heme proteins—a long-standing problem. These spectra can be understood in terms of varying contributions from two electronic states of the same heme complex, mediated via perturbation of the ligand geometry by the rest of the protein.

Quantum mechanical elucidation of the electronic structure of nitrosylheme complexes is an important problem that is relevant to our understanding of the heme environment and its function in various heme proteins. Complexes of the nonbiological NO ligand with hemoglobin and myoglobin,[1-13] and with various model heme systems[14-18] have been the subject of extensive spectroscopic studies in recent years. This intense interest stems from the implicit assumption that the electronic structures of nitrosyl- and oxyhemoglobin—except for the presence of an unpaired electron in the case of NO—are similar, so that the nitrosyl complex serves as a paramagnetic model for the physiologically important, but diamagnetic, oxyhemoglobin. This assumption, however, is primarily deduced from the observed similarities of geometry,[19-23] cooperativity of binding,[24-26] and quantum yield of photodissociation[27,28] for the two ligands and not any rigorous comparison of the electronic structures of their respective complexes. It is worth noting that similar deductions have also led to other simplified electronic models in the literature, notably the isoelectronic model of Hoffman and Gibson,[29] for correlating the quantum yield of photodissociation of diatomic CO, NO, and O_2 molecules from heme complexes.

Clearly, a complete understanding of nitrosyl-heme bonding and the extent to which it can be used as a model for the physiological O_2 ligand require a detailed elucidation of its electronic structure. However, unlike oxy- and carbonylheme complexes, molecular orbital studies of nitrosyl ferrous heme, partly due to its open-shell nature, have been scarce and limited to only CCEH (charge consistent extended Hückel) treatments.[30,31] Accordingly, most of the present conclusions about the electronic structure of NO complexes are derived from the interpretation of the EPR,[1-7,9,10,15-18,32] Mössbauer,[12-14] optical,[8,16,32] and resonance Raman[10,33] data. EPR spectra of nitrosylheme complexes have been, by far, the most widely studied.[1-7,15-18] It is a measure of success of the EPR studies that, through the use of the characteristic g values and hyperfine spectra of myoglobin and hemoglobin nitroxide[1-7] and the sensitivity of the spectra to the nature of the ligand trans to NO,[17,18,32] it was correctly established that the imidazole group of a histidine residue is the proximal ligand in cytochrome c and horseradish peroxidases but not in catalase.[32] In spite of such successful predictions, however, EPR studies have also given rise to a number of controversial and unresolved questions, particularly, about the nature of nitrosyl bonding and the extent of delocalization of the unpaired electron over the metal and the axial ligand orbitals.

A commonly postulated interpretation of the EPR g values and hyperfine data[1-4,7,16,17] for nitrosyl ferrous heme proteins is based on significant delocalization of the unpaired electron density into the iron d_{z^2} orbital. However, there is considerable disagreement about the nature and extent of the electron spin delocalization obtained from the analysis of different EPR spectra from various heme sources and under differing experimental conditions.[1-4,7] Calculations of the g values and hyperfine coupling constants using only iron d_{z^2} and d_{yz} and NO $2p_\pi^*$ orbitals[33,34] and CCEH mo-

† The Rockefeller University.
‡ SRI International.

(1) Kon, H. *J. Biol. Chem.* **1968**, *243*, 4350-4357.
(2) Chien, J. C. W. *J. Chem. Phys.* **1969**, *51*, 4220-4227.
(3) Dickinson, L. C.; Chien, J. C. W. *J. Am. Chem. Soc.* **1971**, *93*, 5036-5040.
(4) Dickinson, L. C.; Chien, J. C. W. *Biochem. Biophys. Res. Commun.* **1974**, *59*, 1292-1297.
(5) Henry, Y.; Banerjee, R. *J. Mol. Biol.* **1973**, *73*, 469-482.
(6) Doetschman, D. C.; Utterback, S. G. *J. Am. Chem. Soc.* **1981**, *103*, 2847-2852.
(7) Hori, H.; Ikeda-Saito, M.; Yonetani, T. *J. Biol. Chem.* **1981**, *256*, 7849-7855.
(8) Nagai, K.; Hori, H.; Morimoto, H.; Hayashi, A.; Taketa, F. *Biochemistry* **1979**, *18*, 1304-1308.
(9) Nagai, K.; Hori, H.; Yoshida, S.; Sakamoto, H.; Morimoto, H. *Biochim. Biophys. Acta* **1978**, *532*, 17-28.
(10) Scholler, D.; Wang, M.-Y. R.; Hoffman, B. M. *J. Biol. Chem.* **1979**, *254*, 4072-4078.
(11) Maxwell, J. C.; Caughey, W. S. *Biochemistry* **1976**, *15*, 388-396.
(12) Lang, G.; Marshall, W. *Proc. Phys. Soc., London* **1966**, *87*, 3-34.
(13) Lang, G.; Marshall, W. *J. Mol. Biol.* **1966**, *18*, 385-404.
(14) Oosterhuis, W. T.; Lang, G. *J. Chem. Phys.* **1969**, *50*, 4381-4387.
(15) Morse, R. H.; Chan, S. I. *J. Biol. Chem.* **1980**, *255*, 7876-7882.
(16) Wayland, B. B.; Olson, L. W. *J. Am. Chem. Soc.* **1974**, *96*, 6037-6041.
(17) Kon, H.; Kataoka, N. *Biochemistry* **1969**, *8*, 4757-4762.
(18) Kobayashi, K.; Tamura, M.; Hayashi, K. *Biochim. Biophys. Acta* **1982**, *702*, 23-29.
(19) Deatherage, J. F.; Moffat, K. *J. Mol. Biol.* **1979**, *134*, 401-417.
(20) Piciulo, P. L.; Rupprecht, G.; Scheidt, W. R. *J. Am. Chem. Soc.* **1974**, *96*, 5293-5295.
(21) Scheidt, W. R.; Piciulo, P. L. *J. Am. Chem. Soc.* **1976**, *98*, 1913-1919.
(22) Scheidt, W. R.; Frisse, M. E. *J. Am. Chem. Soc.* **1975**, *97*, 17-21.
(23) Scheidt, W. R.; Brinegar, A. C.; Ferro, E. B.; Kirner, J. F. *J. Am. Chem. Soc.* **1977**, *99*, 7315-7322.
(24) Gibson, Q. H.; Roughton, F. J. W. *Proc. R. Soc. London* **1957**, *B147*, 44-56.
(25) Cassoly, R.; Gibson, Q. H. *J. Mol. Biol.* **1975**, *19*, 301-313.
(26) Gibson, Q. H.; Hoffman, B. M. *J. Biol. Chem.* **1979**, *254*, 4691-4697.
(27) Gibson, Q. H.; Ainsworth, S. *Nature (London)* **1957**, *180*, 1416-1417.
(28) Saffran, W. A.; Gibson, Q. H. *J. Biol. Chem.* **1977**, *252*, 7955-7958.
(29) Hoffman, B. M.; Gibson, Q. H. *Proc. Natl. Acad. Sci. U.S.A.* **1978**, *75*, 21-25.
(30) Loew, G. H.; Kirchner, R. F. *Int. J. Quantum Chem., Quantum Biol. Symp.* **1978**, *5*, 403-415.
(31) Doetschman, D. C. *Chem. Phys.* **1980**, *48*, 307-314.
(32) Yonetani, T.; Yamamoto, H. In *Oxidases and Related Enzyme Systems*; King, T. E., Mason, H. S., Morrison, M., Eds.; University Press: Baltimore, MD, 1973; pp 279-298.
(33) Kitagawa, T.; Kyogoku, Y.; Iizuka, T.; Saito, M. I. *J. Am. Chem. Soc.* **1976**, *98*, 5169-5173.

0002-7863/89/1511-2767$01.50/0

lecular orbitals[35] have been reported but have not resolved the conflicting aspects of the experimental observations. The observed in-plane anisotropy of the EPR spectra has been interpreted in terms of the interaction of the iron d_π with the N_ϵ nitrogen p_π orbitals of the proximal imidazole.[7,30,36] The N(Im) spin density is estimated to be of the order of 5% with little or no spin distribution over the porphyrin pyrrole nitrogens.[4]

Besides uncertainties in the electron spin distribution, the EPR data have also left unresolved questions about the axial ligand geometries. An Fe–N–O bond angle of 110°[2,3] determined from the analysis of the EPR data at 77 K is quite different from the value of 145° determined from the X-ray data.[19] An added complication is an observed temperature dependence of the EPR spectra. Hori et al.[7] have obtained different EPR spectra of myoglobin nitroxide at 77 K and 20 °C and have suggested two corresponding high- and low-temperature Fe–NO geometries to account for this difference. A thermal equilibrium of two species has also been suggested[15] as a means of reproducing various other heme protein EPR data.

In this paper, we present the results of a generalized open-shell INDO-RHF treatment[37] of the ground-state electronic structure of nitrosyl ferrous heme. These results clearly indicate the existence of two distinct, nearly degenerate, low-energy electronic states, corresponding to the formal assignment of the unpaired electron to the NO or iron atomic orbitals, respectively. We further show that the energy separation, relative ordering, and mixing of these two states can be achieved via the stretching or bending modes of the axial ligands. The implication of these results is very important in that they provide an alternative interpreation of the observed EPR spectra of NO complexes with various heme proteins, eliminating the need to invoke two species. Instead, the EPR behavior can be understood in terms of thermal or electronic mixing of two electronic states of the same species, mediated through the perturbation of the ligand geometry by the rest of the protein.

Methods

The calculations were carried out with a semiempirical INDO/S (intermediate neglect of differential overlap) program,[37,38] with spectroscopic parameterization, which allows for the treatment of transition-metal complexes. The program includes a restricted Hartree–Fock formalism (RHF), and the self-consistent-field (SCF) calculations are performed by using a generalized open-shell operator.[37] In contrast to unrestricted Hartree–Fock (UHF), an RHF treatment is free of spin contaminations and is suitable for configuration interactions in spectra calculations. Thus, it allows for an even-handed treatment of the ground and excited states of open-shell heme complexes, independent of their oxidation and spin states.

The geometry of the 6-coordinate nitrosylheme was obtained from the X-ray crystal geometry of FeTPP(NMeIm)NO,[20,21] with the porphyrin ring portion of the complex regularized to D_{4h} symmetry and all peripheral substituents replaced by hydrogens. In this geometry, the iron is out of the porphyrin plane by 0.07 Å and the Fe–N bond distances are 1.743 and 2.180 Å for the NO and imidazole ligands, respectively.[20,21]

Over 50 ground-state calculations were carried out by incrementally varying the iron–axial ligand distances from the above geometry and for different values of the NO azimuthal angle, Fe–N–O bond angle, and out-of-plane distance of iron. In each case, convergence to one of the two distinct electronic states was achieved by using a simple Hückel density matrix as the starting point of the SCF calculations. Alternatively, a previously calculated set of eigenvectors could be used as the starting vectors for a new incrementally varied geometry in order to selectively force convergence to a similar state. When these two procedures were used, convergence to two energetically distinct electronic states could be obtained for almost all geometries considered. The exception occurred for a geometry corresponding to an approximate 90° Fe–N–O bond angle, with NO nitrogen off-axis. In this instance, only one state was obtained, independent of the nature of the starting eigenvectors.

Results

One of the characteristic features of the EPR spectra of nitrosylheme complexes is that the hyperfine spectra of both model 5-coordinate[15–17] and modified or denatured heme protein[1,8–11] complexes are distinguishable from those of 6-coordinate or intact protein complexes with nitrogenous bases. The coordination dependence of the hyperfine splitting is considered important in determining the extent of delocalization of the unpaired electron between iron and NO nitrogen orbitals. In our early attempts to calculate the electronic structures of 5- and 6-coordinate complexes, we noted that each converged to a different electronic state, distinguished primarily by the assignment of the unpaired electron to either iron or NO orbitals. In order to determine whether these results were the consequence of the coordination number or whether both states were present in 5- and 6-coordinated species, the following sets of calculations were carried out. In one set, the eigenvectors of the final state of the 6-coordinate complex at the equilibrium geometry were used as the starting vectors in a series of SCF calculations corresponding to an incremental increase of 0.5 Å in iron–imidazole distance. In each calculation, eigenvectors obtained were used as the starting vectors for the next incremental increase of Fe–N(Im) distance. This procedure was repeated until Fe–N(Im) was long enough (11.68 Å) that the complex could be considered 5-coordinated. A similar procedure was followed in reverse order by a stepwise decrease of the iron–imidazole distance starting from the 5-coordinate geometry. In this way, convergence was obtained to two distinct electronic states for both 5- and 6-coordinate nitrosylheme complexes. For convenience of discussion, the two reference states are labeled as ref_{Fe} and ref_{NO} to reflect the site of the unpaired electron localization.

Table I shows the energies and major components of the molecular orbitals for these two reference states in a 6-coordinate nitrosylheme complex at Fe–N(NO) and Fe–N(Im) distances of 1.743 and 2.180 Å, where D_{4h} symmetry designations are used to refer to the porphyrin π orbitals. Table II shows the same results for an effectively 5-coordinate complex, where Fe–N(Im) = 11.68 Å. The singly occupied orbitals (79) are not the highest occupied molecular orbitals, as noted by their tabulated energies, due to their partial iron d orbital character. However, these MOs are shown between the doubly occupied and virtual orbitals for convenience of identification. Comparison of the ref_{NO} and ref_{Fe} states in Tables I and II shows that the dominant signature of each state is primarily reflected in the character of its singly occupied orbital. Also, while the porphyrin-dominated orbitals remain virtually unaffected in going from the ref_{NO} to ref_{Fe} state, the energies of the MOs with iron d atomic orbital character are decreased by about 0.03 au, accompanied by a similar increase in the energies of MOs with NO π character.

Calculated relative energies of ref_{NO} to ref_{Fe} shows that these states are oppositely ordered in 5- and 6-coordinate complexes with $\Delta E = \epsilon_{ref_{Fe}} - \epsilon_{ref_{NO}}$ of −2 and +3 kcal/mol, respectively. In principle, one should be able to obtain the higher energy state from a post-SCF configuration interaction (CI) treatment of the lower energy ground state. However, such states could not be found among the excited states obtained from single-excitation-only CI calculations. Examination of the molecular orbitals in Tables I and II reveals that inclusion of double and higher order excitations will be necessary to provide sufficient configuration mixing to lower the energy of such a state. Unfortunately, CI calculations involving more than a limited set of single excitation configurations in open-shell systems are beyond the present computational capabilities for a restricted Hartree–Fock treatment of systems as large as nitrosylheme complexes. In view of the CI difficulties, it is fortuitous that the sensitivity of these states to axial ligand distances in nitrosylheme has allowed their identification at the SCF

(34) Doetschman, D. C.; Schwartz, S. A.; Utterback, S. G. *Chem. Phys.* **1980**, *49*, 1–8.
(35) Mishra, K. C.; Mishra, S. K.; Roy, J. N.; Ahmad, S.; Das, T. P. *J. Am. Chem. Soc.* **1985**, *107*, 7898–7904.
(36) Yonetani, T.; Yamamoto, H.; Erman, J. E.; Leigh, J. S.; Reed, G. H. *J. Biol. Chem.* **1972**, *247*, 2447–2455.
(37) (a) Edwards, W. D.; Weiner, B.; Zerner, M. C. *J. Am. Chem. Soc.* **1986**, *108*, 2196–2204. (b) Edwards, W. D.; Zerner, M. C. *Theor. Chim. Acta* **1987**, *72*, 347–361.
(38) (a) Ridley, J.; Zerner, M. *Theor. Chim. Acta* **1973**, *32*, 111–134. (b) Ridley, J. E.; Zerner, M. C. *Theor. Chim. Acta* **1976**, *42*, 223–236. (c) Bacon, A. D.; Zerner, M. C. *Theor. Chim. Acta* **1979**, *53*, 21–54. (d) Zerner, M. C.; Loew, G. H.; Kirchner, R. C.; Muller-Westerhoff, U. T. *J. Am. Chem. Soc.* **1980**, *102*, 589–599.

Table I. Ground-State Molecular Orbitals of 6-Coordinate Ferrous Nitrosylheme Complexes[a]

orbital no.	ref_{NO}		ref_{Fe}	
	energy, au	character	energy, au	character
92	0.1014	(94% Imid σ, 3% Imid π)*	0.0974	(93% a_{1u}, 7% Imid σ)*
91	0.1000	(99% a_{1u})*	0.0967	(88% Imid σ, 3% Imid π)*
90	0.0911	(100% e_g)*	0.0880	(100% e_g)*
89	0.0908	(99% e_g)*	0.0878	(99% e_g)*
88	0.0734	(48% $d_{x^2-y^2}$, 31% b_{1u}, 20% Porph σ)*	0.0659	(98% b_{1u})*
87	0.0714	(67% d_{z^2}, 10% Imid σ, 10% Porph σ, 6% NO σ)*	0.0608	(99% Imid π)*
86	0.0673	(68% b_{1u}, 22% $d_{x^2-y^2}$, 9% Porph σ)*	0.0394	(70% $d_{x^2-y^2}$, 28% Porph σ)*
85	0.0656	(98% Imid π)*	0.0359	(51% d_{z^2}, 26% NO $\sigma\pi$, 9% Porph σ, 6% Imid σ)*
84	0.0292	(99% Imid π)*	0.0343	(88% NO π, 5% d_π, 3% Imid π)*
83	0.0227	(100% b_{2u})*	0.0239	(97% Imid π, 3% NO π)*
82	−0.0111	(85% NO π, 12% d_π)*	−0.0201	(100% b_{2u})*
81	−0.0373	(99% e_g)*	−0.0409	(99% e_g)*
80	−0.0379	(99% e_g)*	−0.0413	(99% e_g)*
79	−0.3294	(62% NO π, 27% NO σ, 7% d_π, 4% d_{z^2})*	−0.3541	(76% d_π, 10% d_{z^2}, 7% NO π, 2% NO σ)*
78	−0.2281	100% a_{1u}	−0.2309	100% a_{1u}
77	−0.2389	98% a_{2u}	−0.2420	97% a_{2u}
76	−0.2925	48% d_π, 45% e_g, 7% NO π	−0.2738	41% NO π, 18% NO σ, 12% d_π, 10% d_{z^2}, 15% e_g
75	−0.3009	56% e_g, 41% d_π	−0.3083	62% e_g, 36% d_π, 2% NO π
74	−0.3248	75% d_{xy}, 14% Imid π, 9% b_{1u}	−0.3292	49% Imid π, 50% b_{1u}
73	−0.3252	46% Imid π, 31% b_{1u}, 21% d_{xy}	−0.3346	87% a_{2u}, 10% Imid π
72	−0.3310	73% b_{1u}, 24% Imid π	−0.3358	63% b_{1u}, 36 Imid π
71	−0.3322	85% a_{2u}, 12% Imid π	−0.3421	77% e_g, 7% d_{xy}, 8% NO $\sigma\pi$, 3% d_π
70	−0.3489	94% e_g, 3% d_π, 2% Imid π	−0.3508	80% d_{xy}, 12% e_g
69	−0.3497	99% e_g	−0.3521	96% e_g, 3% d_{xy}
68	−0.3515	56% e_g, 28% d_π, 9% Imid π, 7% NO π	−0.3525	97% e_g, 2% d_{xy}
67	−0.3598	46% d_π, 46% e_g, 6% NO $\sigma\pi$	−0.3630	47% d_π, 35% e_g, 10% Imid π, 8% NO π
66	−0.3993	56% Imid π, 34% Porph σ	−0.4027	52% Imid π, 39% Porph σ

[a] Porphyrin symmetry designations refer to the orbitals in D_{4h} symmetry.

Table II. Ground-State Molecular Orbitals of 5-Coordinate[a] Ferrous Nitrosylheme Complexes[b]

orbital no.	ref_{NO}		ref_{Fe}	
	energy, au	character	energy, au	character
91	0.0942	(100% Imid π)*	0.0933	(100% Imid π)*
90	0.0935	(100% a_{1u})*	0.0912	(100% a_{1u})*
89	0.0834	(100% e_g)*	0.0809	(100% e_g)*
88	0.0832	(100% e_g)*	0.0806	(100% eg)*
87	0.0604	(94% b_{1u}, 4% $d_{x^2-y^2}$)*	0.0569	(99% b_{1u})*
86	0.0563	(100% Imid π)*	0.0555	(100% Imid π)*
85	0.0485	(67% $d_{x^2-y^2}$, 27% Porph σ)*	0.0229	(70% $d_{x^2-y^2}$, 29% Porph σ)*
84	0.0258	(68% d_{z^2}, 17% Fe σ, 6% NO σ)*	0.0139	(100% b_{2u})*
83	0.0161	(100% b_{2u})*	0.0028	(91% NO π, 6% d_π)*
82	−0.0328	(86% NO π, 10% d_π)*	−0.0077	(40% d_{z^2}, 16% NO π, 16% NO σ, 12% Fe σ, 6% d_π)*
81	−0.0457	(98% e_g, 1% d_π)*	−0.0485	(99% e_g)*
80	−0.0458	(99% e_g)*	−0.0485	(99% e_g)*
79	−0.3519	(61% NO π, 26% NO σ, 7% d_π, 5% d_{z^2})*	−0.3834	(74% d_π, 15% d_{z^2}, 4% NO π, 3% d_{xy})*
78	−0.2359	100% a_{1u}	−0.2382	96% a_{1u}
77	−0.2516	97% a_{2u}, 1% d_{z^2}	−0.2549	96% a_{2u}, 1% NO π
76	−0.3042	100% Imid π	−0.2980	37% NO π, 21% NO σ, 16% d_{z^2}, 15% e_g, 10% d_π
75	−0.3112	59% e_g, 37% d_π, 4% NO π	−0.3050	100% Imid π
74	−0.3173	69% e_g, 29% d_π	−0.3191	67% e_g, 31% d_π
73	−0.3380	100% b_{1u}	−0.3407	100% b_{1u}
72	−0.3473	53% a_{2u}, 43% d_{xy}	−0.3501	89% a_{2u}, 6% d_{xy}, 4% NO $\pi\sigma$
71	−0.3487	52% d_{xy}, 44% a_{2u}	−0.3540	82% Porph π, 9% NO $\pi\sigma$, 5% d_π, 4% d_{z^2}
70	−0.3569	100% e_g	−0.3593	100% e_g
69	−0.3570	100% e_g	−0.3597	100% e_g
68	−0.3728	46% d_π, 43% e_g, 10% NO π	−0.3685	85% d_{xy}, 1% Porph $\pi\sigma$
67	−0.3734	100% Imid π	−0.3742	100% Imid π
66	−0.3744	98% Imid σ	−0.3753	98% Imid σ
65	−0.3808	58% d_π, 33% e_g, 8% NO $\sigma\pi$	−0.3799	55% d_π, 34% e_g, 10% NO $\sigma\pi$

[a] Fe–N(1m) = 11.68 Å. [b] Porphyrin symmetry designations refer to π orbitals in D_{4h} symmetry.

level. From the stability of the SCF convergence for all the cases examined, we can conclude with certainty that the calculated reference states in each case correspond to stationary states at the SCF level.

The existence of two distinct electronic states in NO heme provides an alternative interpretation of the EPR spectra, eliminating the need to invoke two different species as previously assumed. Instead, the spectra can be understood on the basis of a thermal distribution or mixing of two electronic states of a single species. In this context, two questions of interest are the following: (1) how the order and degeneracy of the states are affected by changes in the axial ligand geometry, and (2) whether any mixing of the two states can result from such ligand geometry changes. To this end, numerous calculations were carried out as a function of the out of planarity of the iron, NO rotation, Fe–N–O bond angle, and various combinations of Fe–N(NO) and Fe–N(Im) distances. The primary effect of the NO rotation at crystal Fe–N–O bond angles is a change in anisotropy of d_π population, i.e., d_{xz} versus d_{yz} occupancy, with little effect on any other aspect of the two reference electronic states. Similarly, out-of-plane

Table III. Calculated Ground-State Electronic Properties of Ferrous Nitrosylheme Complexes

Fe–N, Å		d orbital spin[a]		net spin				charge	
N(Im)	N(NO)	d_{z^2}	d_π	N(NO)	N(Im)	Fe	NO	Fe	NO
				ref_{NO}					
2.18	1.74	0.04 (0.36)	0.06 (3.63)	0.57	0.002	0.10	0.88	+1.18	−0.26
2.58	1.74	0.04 (0.32)	0.07 (3.64)	0.56	0.000	0.11	0.88	+1.11	−0.24
3.08	1.74	0.05 (0.31)	0.07 (3.65)	0.56	0.000	0.12	0.88	+1.10	−0.23
6.68	1.74	0.05 (0.30)	0.07 (3.66)	0.56		0.12	0.88	+1.10	−0.22
6.68	1.84	0.03 (0.24)	0.05 (3.76)	0.59		0.08	0.91	+1.04	−0.14
2.18	1.94	0.02 (0.26)	0.03 (3.80)	0.66	0.000	0.05	0.94	+1.06	−0.10
2.18[b]	1.74	0.00 (0.30)	0.04 (3.67)	0.62	0.000	0.05	0.94	+1.21	−0.37
2.18[c]	1.74	convergence to ref_{Fe} only							
				ref_{Fe}					
2.18	1.74	0.10 (0.76)	0.77 (3.05)	0.07	0.003	0.88	0.10	+1.27	−0.46
2.58	1.74	0.13 (0.81)	0.76 (3.01)	0.05	0.002	0.91	0.07	+1.18	−0.42
3.08	1.74	0.14 (0.84)	0.75 (3.00)	0.04	0.001	0.92	0.06	+1.15	−0.39
6.68	1.74	0.15 (0.87)	0.74 (2.99)	0.04		0.92	0.05	+1.14	−0.37
6.68	1.84	0.12 (0.84)	0.78 (3.02)	0.02		0.94	0.03	+1.10	−0.35
2.18	1.94	0.05 (0.73)	0.84 (3.05)	0.03	0.001	0.93	0.04	+1.18	−0.42
2.18[b]	1.74	0.43 (0.83)	0.41 (3.08)	0.09	0.011	0.85	0.12	+1.23	−0.40
2.18[c]	1.74	0.38 (0.91)	0.54 (3.00)	0.01	0.010	0.93	0.03	+1.27	−0.45

[a] Numbers in parentheses refer to corresponding d orbital populations. The d_{xy} orbital population is 2.0 in all geometries. [b] 20 °C geometry in ref 7. [c] 77 K geometry in ref 7.

movement of iron to either side of the porphyrin plane has only a minor effect on the overall description of the two electronic states. On the other hand, profound effects on the relative order and the extent of degeneracy of the two states were observed with variations in axial ligand distances and Fe–N–O bond angle.

Figure 1 shows the changes in the energy difference $\Delta E = ref_{Fe} - ref_{NO}$) as a function of Fe–N(Im) distance for several parametric Fe–N(NO) distances. The asymptotic behavior of the data at the 5-coordination limit indicates that, for Fe–N(NO) distances of greater than about 1.8 Å, ref_{NO} is always more stable than the ref_{Fe} state. At shorter Fe–N(NO) distances, the relative order can be reversed by varying the Fe–N(Im) distance. At the crystal Fe–N(NO) distance of 1.743 Å, ref_{NO} is more stable than ref_{Fe} at Fe–N(Im) distances of less than 2.5 Å. Thus, an increase of about 0.5 Å from the equilibrium Fe–N(Im) distance can result in the reversal of the order of the two states.

Hori et al.[7] have suggested two different ligand geometries for myoglobin nitroxide at 20 °C and 77 K. These geometries were also investigated in this study. The proposed high-temperature geometry is similar to the X-ray structure except for the rotation of Fe–N–O by 20° away from the z axis. The relative energy and order of the two reference states calculated for this geometry was similar to that obtained for the crystal geometry with the ref_{NO} state being lower in energy by about 5 kcal/mol than the ref_{Fe} state. The proposed low-temperature geometry involves an Fe–N–O angle of 110° with Fe–N(NO) being off-axis by 30° such that the N–O is located approximately above the iron. Calculations in which Fe–N–O is further bent from the crystal value of 145° to 110°, with nitrogen retained on the z axis, result in the stabilization of ref_{Fe} relative to ref_{NO}, but convergence to both electronic states is still possible. However, when Fe–N(NO) is placed off-axis by 30°, only a ref_{Fe}-type state could be obtained, independent of the starting eigenvectors. Specifically, all attempts to converge on a ref_{NO}-type state using ref_{NO}-type eigenvectors from other closely related geometries as the starting state resulted in a slow convergence to a ref_{Fe} state.

Table III shows selected orbital populations, spin distributions, and net charges at several representative geometries for ref_{NO} and ref_{Fe} states. Only the calculated iron d_{z^2} and d_π orbital spins and populations are shown. The d orbital populations averaged over the geometries in Table III are $(d_{z^2})^{0.3}(d_{x^2-y^2})^{0.4}(d_{xy})^{2.0}(d_\pi)^{3.7}$ for ref_{NO} and $(d_{z^2})^{0.8}(d_{x^2-y^2})^{0.5}(d_{xy})^{2.0}(d_\pi)^{3.0}$ for ref_{Fe} state. However, the near unit electron occupancy of d_{z^2} orbital in ref_{Fe} is effectively spin-paired, and the unpaired spin is primarily in the d_π orbitals. Indeed, only when N(NO) is off-axis, as shown for the geometries proposed by Hori et al.,[7] is the spin localization in the d_{z^2} orbital comparable to that in the d_π orbital. Although the calculated net spins indicate 90% spin localization on NO for ref_{NO} and on Fe for the ref_{Fe} state, the calculated net charges are not nearly as sensitive to the change of state and are even less sensitive to changes in the ligand geometry within each state.

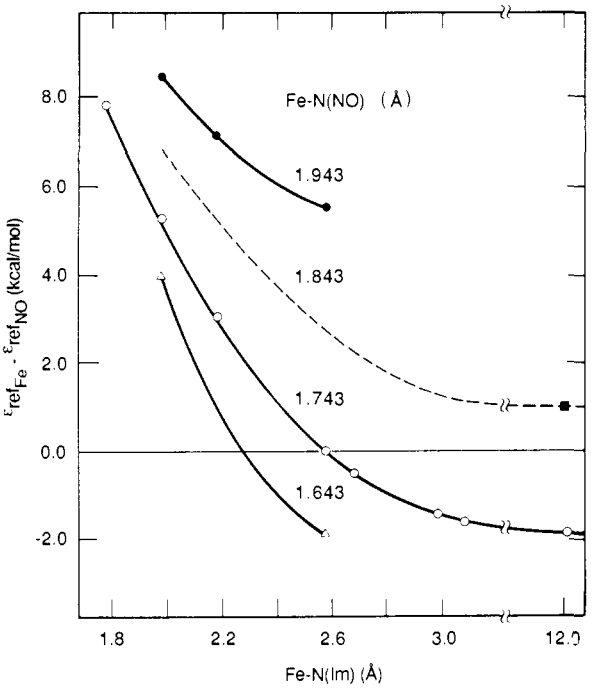

Figure 1. Calculated $\Delta E = ref_{Fe} - ref_{NO}$ as a function of Fe–N(Im) distance for different Fe–N(NO) distances.

Table IV shows the calculated values of the principal component of the electronic field gradient, V_{max}, the asymmetry parameter, η, and the Mössbauer zero-field quadrupole spitting ΔE_Q for the complexes shown in Table III. Also included in Table IV are the calculated isotropic and anisotropic principal components for ^{57}Fe hyperfine constants observed in ESR spectra. The corresponding internal magnetic field at the ^{57}Fe nucleus in Mössbauer spectra are also given.

Discussion

The major result of the present study is the demonstration of the existence of two low-energy electronic states in nitrosyl ferrous heme complexes. These two states are nearly degenerate at axial ligand distances close to those observed in heme protein complexes.[19-22] Furthermore, both the energy difference and the relative order of the two electronic states can be changed by only minor variations in the axial ligand distances and bond angles.

The existence of two nearly degenerate electronic states has important implications for the interpretation of the spectroscopic

Table IV. Calculated Quadrupole Splitting and Hyperfine Constants for Ferrous Nitrosylheme Complexes

Fe–N, Å		quadrupole splitting			isotropic and anisotropic hyperfine (internal field)			
N(Im)	N(NO)	ΔE_Q, mm/s	η	V_{max}, au	isototropic, MHz (KG)	A_{xx}, MHz (KG)	A_{yy}, MHz (KG)	A_{zz}, MHz (KG)
					ref_{NO}			
2.18	1.74	1.03	0.64	0.75	−2.57 (9.3)	−6.92 (25.1)	−2.73 (9.9)	1.94 (−7.1)
2.58	1.74	1.14	0.43	0.86	−2.76 (10.0)	−7.48 (27.2)	−3.00 (10.9)	2.19 (−8.0)
3.08	1.74	1.22	0.33	0.93	−2.81 (10.2)	−7.68 (27.9)	−3.05 (11.1)	2.30 (−8.4)
6.68	1.74	1.27	0.28	0.97	−2.76 (10.0)	−7.58 (27.6)	−3.03 (11.0)	2.34 (−8.5)
6.68	1.84	1.23	0.15	0.95	−1.34 (4.9)	−4.51 (16.4)	−1.60 (5.8)	2.09 (−7.6)
2.18	1.94	0.84	0.28	0.65	−0.39 (1.4)	−2.32 (8.4)	−0.65 (2.3)	1.80 (−6.6)
2.18[a]	1.74	1.35	0.86	0.94	−1.64 (6.0)	−4.11 (14.9)	−2.68 (2.2)	−0.21 (0.8)
2.18[b]	1.74	convergence to ref_{Fe} only						
					ref_{Fe}			
2.18	1.74	1.56	0.34	1.19	−30.08 (109.3)	−66.57 (241.9)	−31.93 (116.0)	8.26 (−30.1)
2.58	1.74	1.45	0.47	1.09	−30.70 (111.6)	−65.83 (239.2)	−37.13 (134.9)	10.88 (−39.5)
3.08	1.74	1.46	0.42	1.10	−30.51 (110.9)	−66.16 (240.5)	−36.78 (133.7)	11.42 (−41.5)
6.68	1.74	1.40	0.57	1.03	−30.25 (109.9)	−64.03 (232.7)	−39.68 (144.2)	12.96 (−47.1)
6.68	1.84	1.42	0.67	1.03	−30.87 (112.2)	−65.15 (236.8)	−40.71 (148.0)	13.25 (−48.1)
2.18	1.94	1.65	0.58	1.22	−31.69 (115.2)	−69.87 (253.9)	−34.84 (126.6)	9.64 (−35.1)
2.18[a]	1.74	1.59	0.98	1.07	−27.61 (100.3)	−62.26 (226.3)	−30.20 (109.6)	9.59 (−34.8)
2.18[b]	1.74	2.00	0.98	1.36	−29.03 (105.5)	−66.92 (243.2)	−32.27 (117.3)	12.10 (−44.0)

[a] 20 °C geometry in ref 7. [b] 77 K geometry in ref 7.

properties of nitrosylheme complexes, particularly with respect to the use of NO as a paramagnetic model for the diamagnetic oxyheme. Our present results indicate that convergence to two separate electronic states can be obtained for a wide range of variations in the axial ligand geometry. Although energy crossing between the two states is obtained only in the case of severe bending of the NO ligand when it is off-axis, the extent of degeneracy and the order of the states are very sensitive to variations in the Fe–N(Im) distance near its observed equilibrium values. Therefore, mixing of the two electronic states may very likely occur via minor perturbations of the axial ligand geometries mediated by the stretching and bending modes of the ligands. Without higher order CI calculations at each specific geometry, our SCF results cannot distinguish between electronic or thermal mixing of the two reference states. However, independent of either possibility, our results provide an alternative interpretation of the observed EPR spectra in terms of contributions from two low-lying electronic states of a single species as opposed to contributions from two different species, such as suggested by Morse and Chan.[15] Either electronic or thermal mixing of two electronic states is equally consistent with the observed temperature dependence of the EPR spectra.[15]

In view of our results, the observed variations in EPR spectra for heme proteins from various sources and under differing experimental conditions can be accounted for in terms of changes in the ligand geometry, which may be induced by the protein. In particular, the differences in the EPR spectra of myoglobin nitroxide at ambient and below freezing temperatures observed by Hori et al.[7] can be explained in terms of changes in electronic state as a consequence of their proposed geometry changes. Specifically, at their low-temperature geometry, ref_{Fe} is found to be the major component of the electronic structure, indicating maximum delocalization of the unpaired electron into the iron d_{z^2} orbital. On the other hand, their proposed high-temperature geometry results in a preference for the ref_{NO} state, corresponding to spin localization on NO. Therefore, depending on the external conditions, the protein may be able to stabilize one of the two electronic states preferentially and exhibit electronic properties, which originate largely from that state.

It is of interest to examine these reference states in terms of an "ionic" model. Then, on the basis of spin distribution alone, the ref_{Fe} state could be considered a formal [(Fe(III), $S = {}^1/_2$)$(NO)^-$] and the ref_{NO} state a formal [Fe(II)(NO, $S = {}^1/_2$)] state. However, the results summarized in Table III show how the charge redistribution in the complex modulates this ionic description and leads to two states of very similar electronic charges and energies despite differences in spin distributions. Although the spin distributions are consistent with the ionic description, the net charges on the iron and the NO in the ref_{Fe} state are not significantly different from those in the ref_{NO} state. In particular, the net increase in the partial negative charge on NO is less than 0.2e between the ref_{Fe} and ref_{NO} states.

The calculated d orbital electron and spin populations in Table III indicate that the iron in the ref_{Fe} state retains a ferric-like character while the iron in the ref_{NO} state is ferrous-like, despite the similarity of the net atomic charges. The ferric character of the ref_{Fe} state results from the d orbital configuration $(d_{z^2})^{0.8}$-$(d_{x^2-y^2})^{0.4}(d_{xy})^{2.0}(d_\pi)^{3.0}$ where the large spin-paired d_{z^2} population is obtained at the expense of a hole in d_π orbitals, which have become the site of the unpaired spin. The off-axis movement of N(NO) modulates this picture, resulting in the increase of spin localization in the d_{z^2} orbital. This is in sharp contrast to the ref_{NO} state, where the iron environment in the ref_{NO} state is ferrous-like, with nearly 6e in the closed-shell d orbitals and the unpaired spin localized on the NO.

It is interesting that Mössbauer studies cannot definitively distinguish between the ferrous- and ferric-like environments in nitrosylhemoglobin.[12] Although the calculated ΔE_Q for ref_{Fe} states (Table IV) are closer to the experimentally observed value of 1.3–1.5 mm/s,[12,13] an average of the calculated values of the two states is equally consistent with the observed value. It is thus possible that contributions from both the ref_{NO} and ref_{Fe} states could account for the inability of results from Mössbauer resonance studies to distinguish between ferrous- and ferric-like environments. A similar conclusion can be drawn from the comparison of the calculated ^{57}Fe isotropic hyperfine and anisotropic principal components of the hyperfine constant with the observed ESR[32] and Mössbauer[14] spectra. The observed ^{57}Fe isotropic hyperfine for nitric oxide compounds of cytochrome *c* peroxidase and horseradish peroxidase is about 6.5 G (18.2 MHz). The $A_\parallel$ and $A_\perp$ components of the anisotropic hyperfine obtained from the fit to Mössbauer spectra of hemoglobin nitric oxide at an applied field of 500 G[14] are 3.3 G (9.3 MHz) and 9.6 G (26.9 MHz), repectively. These values, although closer in order of magnitude to the calculated hyperfine parameters for the ref_{Fe} state in Table IV, are also consistent with an average of the calculated parameters for the two states.

Finally, as shown in Table III, very small spin densities are calculated for the imidazole nitrogen. Only in the case of the ref_{Fe} state is there a significant increase in the N(Im) spin as a result of off-axis movement of the NO ligand. We have also observed, in a nonrelated study of cytochrome *c* peroxidase,[39] that the spin density on N(Im) is sensitive to the anionicity of the imidazole

(39) Axe, F. U.; Waleh, A.; Chantranupong, L.; Loew, G. H. *Int. J. Quantum Chem.*, in press (proceedings of the WATOC 1987 World Congress).

ligand, such as it may arise from hydrogen bonding of its N^{δ} to nearby polar amino acids. Therefore, the observed hyperfine due to N(Im) may not only depend on the contributions from the electronic states suggested by this study, it may also be sensitive to the ligand geometry and the immediate electronic environment of imidazole.

Acknowledgment. We gratefully acknowledge financial support for this work from NSF Grant PCM 8410244. We also thank the National Science Foundation for a supplement to this grant for the generous use of the San Diego and Pittsburgh Supercomputer Centers. The helpful guidance and support of the staff at these centers is also gratefully acknowledged. A.W. wishes to particularly thank Dr. M. C. Zerner for his encouragement and his suggestions and Dr. J. R. Collins for many hours of helpful discussions.

Jahn-Teller Effects in the Photodissociation of Ozone†

David J. Tannor*

Contribution from the Department of Chemistry, Illinois Institute of Technology, Chicago, Illinois 60616, and The James Franck Institute, University of Chicago, Chicago, Illinois 60637.
Received June 10, 1988

Abstract: The electronic structure of ozone is examined from the viewpoint of the full 3-fold permutational symmetry of the molecule. The three equivalent wells on the ground electronic state potential energy surface are characteristic of a strong second-order Jahn-Teller effect. It is observed that the ground state and the excited electronic state responsible for photodissociation in the Hartley band ($^1A_1$ and $^1B_2$, respectively, in C_{2v}) are partners in an $^1E'$ representation in the D_{3h} molecular symmetry group and are predicted to exhibit a conical intersection at equilateral geometries. Thus, the photoexcitation of ozone in the region 200 to 320 nm may be viewed as a transition from the lower to the upper branch of a Jahn-Teller system. The implications for the dynamics of ozone photodissociation are discussed.

I. Introduction

From spectroscopic data, ozone in its ground electronic state is known to have an isosceles triangle geometry, with a central angle of 116° 47′. This geometry presents an apparent paradox. All three oxygen atoms are equivalent and indistinguishable (barring isotope effects), yet one of the three is singled out as the central atom. The resolution of this paradox and the recovery of the full 3-fold permutational symmetry of the molecule were first discussed in detail by Berry[1] and have been addressed since by several other authors.[2] The resolution involves the existence of three identical minima on the ground electronic state potential energy surface, corresponding to each of the three oxygen atoms occupying the central position. These three "isomers" of ozone may interact with each other by tunnelling, but the time scale for this process in the ground vibronic state, estimated at 10^{90} s[1], is so long that each form can be considered independently for most purposes.

There are, however, situations where the full 3-fold symmetry is indeed important. One case involves highly excited vibrational states of ozone in its ground electronic state, where there is no reason to expect tunnelling contributions to be negligible. Such highly excited vibrational levels can in principle be prepared by direct overtone excitation, multiphoton absorption, or emission from an excited electronic state. A second case involves the excitation to an excited electronic state in which there are no barriers between the different forms of ozone, or in which the barriers are surmountable on chemically significant time scales. Such a situation will be in force in photodissociation of ozone in the Hartley band. In this case interference effects, arising from the different initial forms, are in principle observable. The latter case provides the main motivation for this article.

The present situation provides an example of a molecule that undergoes large amplitude motion. Such molecules, generally termed "floppy", cannot be treated within the framework of conventional point group symmetry. The correct framework for discussing symmetry of floppy molecules was introduced by Longuet-Higgins,[3] and involves the larger permutation-inversion (PI) group of the molecule, a subgroup of which is isomorphic to the point group. The description of vibronic transitions within this larger group involves the following program:[4] (1) relabeling of the electronic states with labels appropriate to the PI group; (2) relabeling of the rovibrational states within the PI group; (3) assignment of a symmetry label to the transition dipole moment within the PI group; and (4) evaluation of allowed transitions to specific rovibronic final states, also labeled within the PI group. There is a fifth step, for excitation to a dissociative electronic state:[5] (5) correlation of the united molecule PI symmetry label with symmetry labels of the fragments.

The new results that emerge from this expanded symmetry treatment may be classified as being of two types, static (electronic) and dynamic (rovibronic). The reassignment of the electronic structure is the subject of section II and yields the following result. The ground electronic state and the excited electronic state responsible for photodissociation in the Hartley band ($^1A_1$ and $^1B_2$, respectively, in C_{2v}) are partners in an $^1E'$ representation in the PI group. There are several intriguing implications of this reassignment: the ground electronic state of ozone, with its three equivalent potential minina, is a classical example of the much sought strong second-order Jahn-Teller effect; the ground and excited state are predicted to exhibit a conical intersection at equilateral geometries; and the photoexcitation of ozone in the Hartley band, which is responsible for the absorption of most of the solar radiation in the range 200 to 320 nm, is a transition from the lower to the upper branch of a Jahn-Teller system.

In section III dynamic effects are discussed. The rovibrational states are relabeled, and several interesting implications for the photoabsorption and final products distributions are considered.

* Address correspondence to the author at the Illinois Institute of Technology.
† Research supported by grants from the PRF (18773-G6) and NSF (CHE-8716122) and an equipment grant from Apple Computer.

(1) Berry, R. S. *Rev. Mod. Phys.* **1960**, *32*, 447.
(2) Kellman, M. *J. Phys. Chem.* **1983**, *87*, 2161.
(3) Longuet-Higgins, H. C. *Mol. Phys.* **1963**, *6*, 445.
(4) Bunker, P. R. *Molecular Symmetry and Spectroscopy*, Academic: London, 1979.
(5) Quack, M. *Mol. Phys.* **1977**, *34*, 477.

0002-7863/89/1511-2772$01.50/0